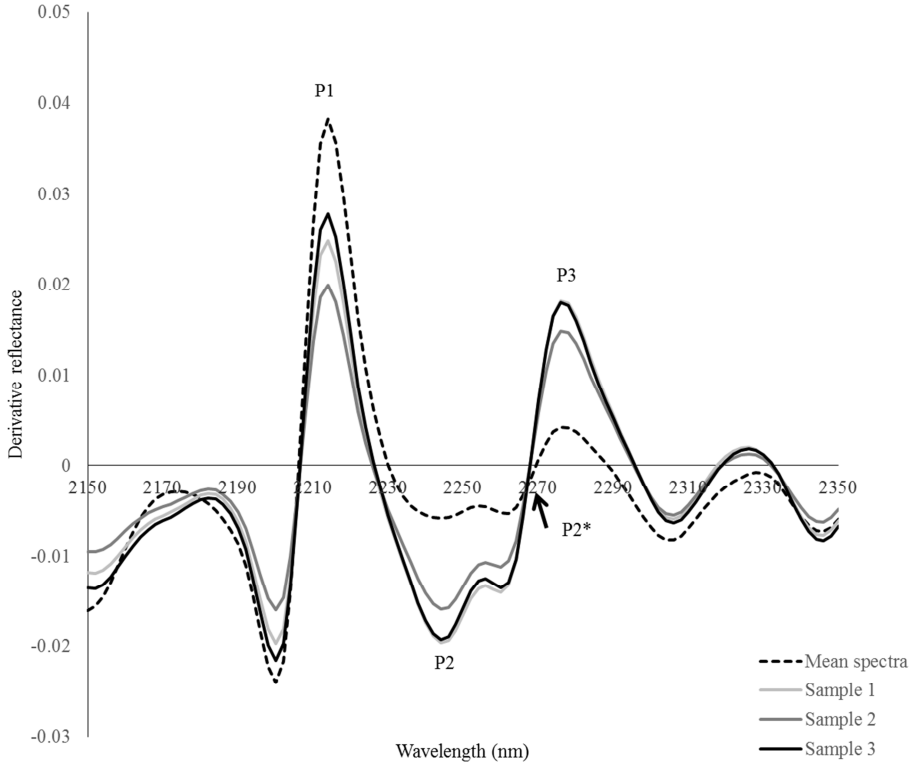

Figure 2. Mean first derivative spectrum of the whole data set and three individual spectra in the 2150-2350 nm range. P1: peak of maximum reflectance of kaolinite, between 2212-2214 nm; P3: peak of maximum reflectance of gibbsite, between 2272-2284 nm; P2: point of minimum reflectance between P1 and P3, situated between 2234 and 2248 nm; P2*: intersection point of the spectra, situated between 2256 and 2268 nm.

3 Results

3.1 Reference soil analyses

The descriptive statistical analyses of mineralogical characteristics of the soils are shown in Table 1. On average, aluminium was the major element (197 ± 83 g kg^{-1} $Al_2O_{3\_SA}$), followed by silicon (142 ± 69 g kg^{-1} SiO_{2_SA}) and iron (80 ± 49 g kg^{-1} $Fe_2O_{3\_SA}$). However, a large variability was observed among the studied soils (Fig. 3a). The mean Ki and Kr ratios, calculated from the SA extraction results, were 1.5 and 1.1, respectively. According to the CPCS (1967), the soils are classified as ferrallitic when Ki < 2. Therefore, 32 soil samples of the 148, including 3 Ferralsols, were not correctly classified based on field observations (Ki > 2).

Kaolinite was the dominant mineral of the clay fraction (305 ± 148 g kg^{-1}) (Table 1 and Fig. 3b). Crystalline iron oxides, estimated by the CBD extraction ($Fe_2O_{3\_CBD}$), accounted for 43 ± 30 g kg^{-1}. The amount of Al_2O_3 in the kaolinite was 227 ± 110 g kg^{-1}

, whereas the amount of Al_2O_3 substituted in the iron oxides was 12 ± 12 g kg^{-1}. The chemical estimation of Al substitution of iron oxides was 33%, i.e. nearly the maximum theoretical Al substitution ratio (Cornell and Schwertmann, 1996). The goethite and hematite contents, calculated from the iron oxide content and Al substitution ratio, were 34 ± 26 g kg^{-1} and 12 ± 18 g kg^{-1}, respectively. The gibbsite content, calculated from the remaining amount of Al_2O_3, was 98 ± 131 g kg^{-1}. The mean R_{KGb} ratio, calculated from the kaolinite and gibbsite contents, was 0.75 ± 0.25.

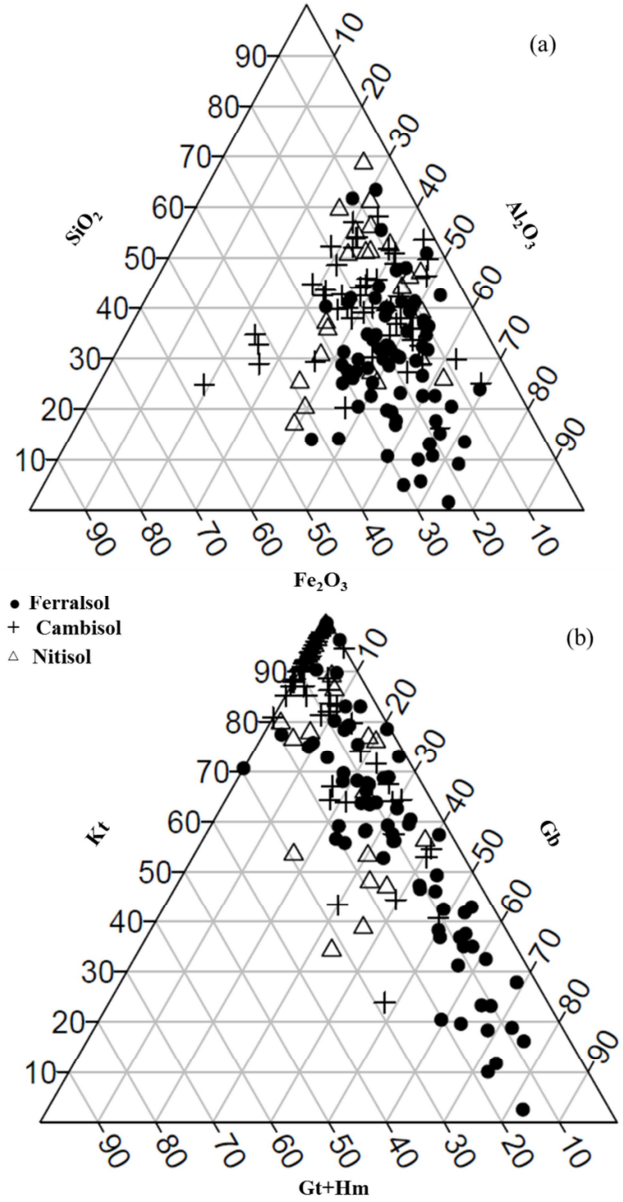

Figure 3. SiO_2, Al_2O_3 and Fe_2O_3 (a) and kaolinite (Kt), gibbsite (Gb) and goethite + hematite (Gt+Hm) (b) relative contents for the Ferralsols, Cambisols and Nitisols studied in Madagascar.

Table 1. Descriptive statistics for mineralogical constituents and ratios of the studied ferralitic soils

Mineralogical constituents / ratios		min	max	mean	SD	median
$Al_2O_{3\_CBD}$	g kg^{-1}	0.5	76.9	12.5	11.7	8.5
$Fe_2O_{3\_CBD}$	g kg^{-1}	0.0	181.4	42.7	30.4	37.4
SiO_{2_SA}	g kg^{-1}	6.2	314.9	141.8	68.8	134.2
$Al_2O_{3\_SA}$	g kg^{-1}	22.0	381.2	196.6	83.1	207.2
$Fe_2O_{3\_SA}$	g kg^{-1}	11.8	231.0	80.2	48.8	70.7
Ki		0.03	4.49	1.46	0.84	1.30
Kr		0.03	3.96	1.15	0.68	1.03
Kaolinite (Kt)	g kg^{-1}	13.3	676.3	304.7	147.9	288.3
Gibbsite (Gb)	g kg^{-1}	0.0	456.2	97.7	131.1	83.8
R_{KGb}		0.03	1.00	0.75	0.25	0.79
Goethite (Gt)	g kg^{-1}	0.0	128.2	33.6	25.8	26.5
Hematite (Hm)	g kg^{-1}	0.0	79.5	12.2	17.9	1.8

$Al_2O_{3\_CBD}$: the amount of Al substituting Fe in iron oxides determined by the citrate-bicarbonate-dithionite (CBD) deferrification method; $Fe_2O_{3\_CBD}$: the amount of Fe determined by the CBD method; SiO_{2_SA}: the amount of silicon determined by the sulfuric acid extraction method (1:1 deionized water/cc. sulphuric acid; SA); $Al_2O_{3\_SA}$: the amount of aluminium determined by the SA method; $Fe_2O_{3\_SA}$: the amount of iron determined by the SA method; Ki: $SiO_{2\_SA}/Al_2O_{3\_SA}$; Kr: $SiO_{2\_SA}/(Al_2O_{3\_SA} + Fe_2O_{3\_SA})$; Kaolinite, Gibbsite, Goethite and Hematite calculated according to Eqs. 1 to 4; R_{KGb}: Kt/(Kt + Gb); SD: standard deviation.

3.2 NIR calibration and validation of mineralogical properties with chemometric methods

The predictions of mineralogical properties of soils using chemometric methods were poorly effective (Table 2). Only $Al_2O_{3\_SA}$ and $Fe_2O_{3\_CBD}$ were satisfactorily calibrated, according to the classification of Chang et al. (2001) and Malley et al. (2004), with R^2_{cv} = 0.74 and 0.80 and RPD_c = 2.0 and 2.2, respectively. All the other mineralogical properties were moderately calibrated (RPD_{cv} between 1.4 and 1.7). External validations also yielded poor results (RPD_v < 2). In the case of kaolinite and gibbsite, the values for the validation set are markedly lower than those of the calibration set (R^2_v = 0.37 and 0.51 and RPD_v = 1.3 and 1.4, respectively).

Table 2. Calibration and validation statistics of modified partial least square (mPLS) regression for the models of prediction by SPIR of several mineralogical constituents and ratios

			Calibration set								Validation set							
Mineralogical constituents Ratios		Pre-treatment of spectra	N	out	n1	Mean	SD	SECV	R^2c	RPD_c	n2	Mean	SD	SEP(c)	Bias	Slope	R^2v	RPD_v
$Al_2O_{3\_CBD}$	g kg^{-1}	MSC 21010	104	7	97	9.9	6.9	4.62	0.56	1.5	42	13.3	5.5	7.98	1.50	1.25	0.43	1.3
$Fe_2O_{3\_CBD}$	g kg^{-1}	MSC 255	104	9	95	36.9	26.0	11.77	0.80	2.2	42	52.3	27.2	21.31	1.40	1.02	0.63	1.6
SiO_{2_SA}	g kg^{-1}	NONE 244	104	5	99	144.0	68.8	44.22	0.60	1.6	42	140.2	59.2	58.42	-13.05	0.72	0.37	1.3
$Al_2O_{3\_SA}$	g kg^{-1}	NONE 001	104	4	100	185.7	81.3	41.90	0.74	2.0	42	223.8	67.1	40.90	0.42	0.99	0.72	1.9
$Fe_2O_{3\_SA}$	g kg^{-1}	SNV 144	104	6	98	74.6	46.8	28.00	0.65	1.7	42	86.3	42.5	45.23	-2.60	0.50	0.22	1.1
Ki		SNV 244	104	4	100	1.5	0.8	0.50	0.60	1.6	42	1.2	0.6	0.52	-0.01	0.94	0.53	1.5
Kr		MSC 001	104	6	98	1.1	0.6	0.40	0.50	1.4	42	1.0	0.4	0.43	-0.08	0.88	0.44	1.3
Kaolinite	g kg^{-1}	NONE 244	104	5	99	309.3	147.8	94.98	0.60	1.6	42	301.2	127.1	125.48	-28.03	0.72	0.37	1.3
Gibbiste	g kg^{-1}	NONE 001	104	34	70	138.4	107.1	67.77	0.60	1.6	34	184.3	92.9	83.51	10.51	0.90	0.51	1.4
R_{KGb}	g kg^{-1}	NONE 001	104	1	103	0.8	0.3	0.20	0.57	1.5	42	0.7	0.3	0.21	-0.02	0.91	0.57	1.5
Goethite	g kg^{-1}	SNV 21010	104	5	99	31.0	23.5	13.97	0.66	1.7	42	38.2	19.5	16.20	3.31	1.04	0.61	1.6
Hematite	g kg^{-1}	NONE 21010	104	51	53	18.1	17.0	9.94	0.66	1.7	33	22.9	12.2	13.10	0.51	1.47	0.70	1.8

Pre-treatment: MSC: Multiplicative Scatter Correction; NONE: no treatment; SNV: Standard Normal Variate. The numbers indicate the derivatives (0, 1 and 2: no derivation, first and second derivatives, respectively); number of point gap (0, 4, 5, 10); number of point for first smoothing (1, 4, 5, 10); and number of point for second smoothing (1); N: total number of samples; out: number of outliers; n1: number of samples in the calibration set (N – out); n2: number of samples in the validation set; Mean: mean of calibration or validation sets; SD: standard deviation; SECV: Standard Error of Cross Validation; R^2_c: coefficient of determination of SECV; RPD_c: Ratio Performance Deviation (SD/SECV); SEP: Standard Error of Prediction; R^2_v: coefficient of determination of SEP. The abbreviations for the mineralogical constituents and ratios are specified in the footnote of Table 1

3.3. NIR calibration and validation of specific spectral peaks for kaolinite and gibbsite

The PLS loadings of the soils spectra (Fig. 4) were analysed after the best pre-treatments made for the four analyzed minerals (Table 2), i.e. NONE 0011 for gibbsite, NONE 2441 for kaolinite, SNV 210101 for goethite and NONE 210101 for hematite. The loadings corresponding to the NONE 0011 pre-treatment had a specific shape with weak and monotonous changes for PC1 and PC2 and a marked peak at nearly 2265 nm for PC3 (Fig. 3a.). For the three other pre-treatments the three loadings were closely identical, with high loadings at 1 350-1 550, 1 850-1 950 and 2 100-2 500 nm (Fig. 4b, 4c, 4d). The most specific spectral bands produced by the studied minerals in the near-infrared range were situated between 2 200 and 2 300 nm. The peak of gibbsite was clearly detected at nearly 2 270 nm with the NONE 0011 pre-treatment, whereas both kaolinite and gibbsite peaks were detected using the NONE 2441 pre-treatment, at nearly 2 205 and 2 270 nm, respectively (Fig. 4b.). Some specific loadings were observed for PC3 at 1 650-1 800 nm with the SNV 210101 pre-treatment that corresponds to the best pre-treatment for goethite (Fig. 4c.).

The correlation, obtained by linear regression between kaolinite content and intensities of its specific absorption peaks (I_{Kt}), and by polynomial regression, between gibbsite content and intensities of specific absorption peaks (I_{Gb}) are shown in Fig. 5. The coefficients of determination were satisfactory for kaolinite and gibbsite, with adjusted R^2_c = 0.69 and 0.71, respectively (Fig. 5.). These coefficients are higher than R^2_c values obtained for kaolinite and gibbsite (0.60) by partial least square regressions (Table 2). The values obtained for the validation set (R^2_v = 0.72, for both kaolinite and gibbsite) are also similar to those of the calibration set.

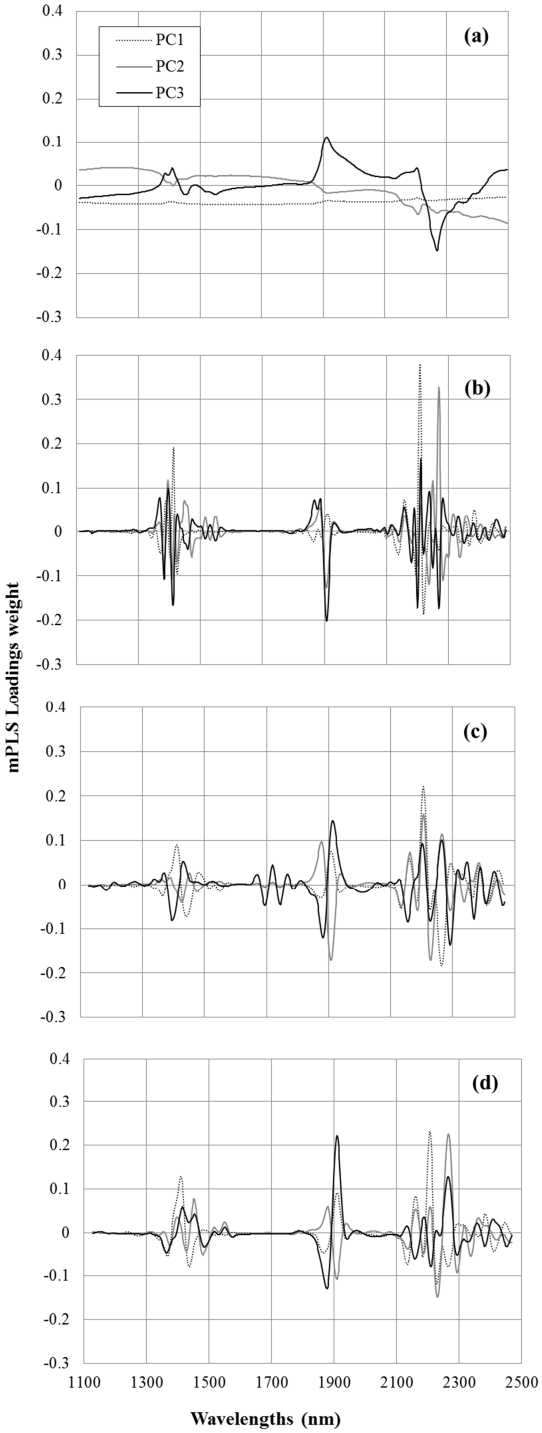

Figure 4. Partial least square loading weights for the PCA transformed NIR reflectance values after the best pre-treatments for the prediction of soil minerals: (a) NONE 0011 for gibbsite; (b) NONE 2441 for kaolinite; (c) SNV 210101 for goethite; (d) NONE 210101 for hematite. NONE: no treatment; SNV: Standard Normal Variate. The numbers indicate the derivatives (0, 1 and 2: no derivation, first and second derivatives, respectively); number of point gap (4, 5, 10); and number of point smoothing (4, 5, 10).

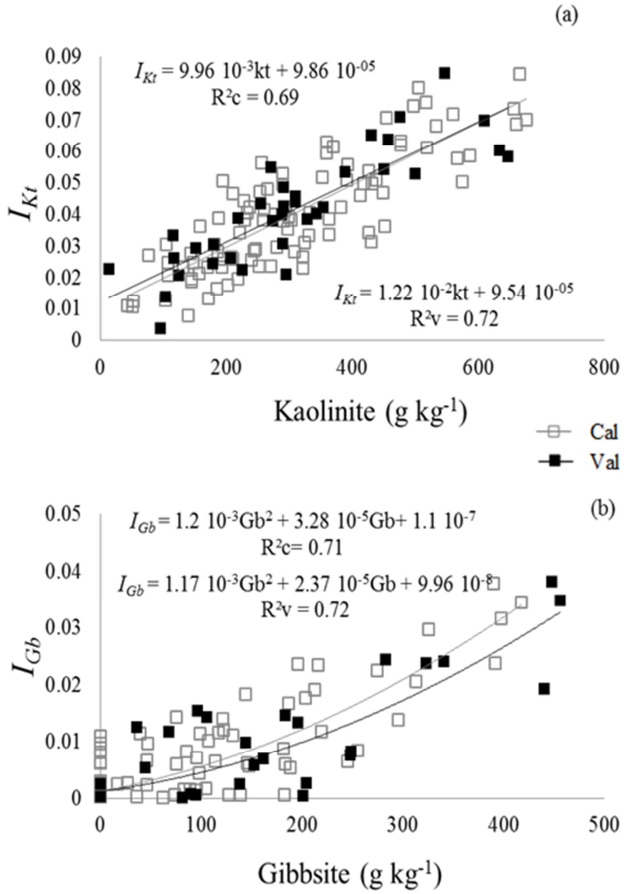

Figure 5. Correlation between absorption intensities of specific peaks for kaolinite (a) and gibbsite (b) and their contents analyzed by wet chemistry. IKt and IGb are the heights of the first derivatives of absorption peaks of kaolinite and gibbsite, respectively.

4 Discussion

4.1 Representativity of the studied soils

The studied soils correspond to ferralitic soils, one of the most common soils group occurring in areas under tropical climate (Adamoli et al., 1985; Dewitte et al., 2013) and represent around 40% of the soils of Madagascar (Roederer, 1971). They have a sand-loam to clayey texture (332 ± 151 g kg^{-1} clay content), that is within the textural variability found in the majority of tropical soils. These soils were formed as the result of intense weathering and, consequently, were highly desilicified, as can be observed by the low Ki and Kr ratios of most of them (Table 1). Kaolinite was the dominant mineral of the clay fraction (305 ± 148 g kg^{-1}), followed by gibbsite, goethite and hematite (98 ± 131; 34 ± 26 and 12 ± 18 g kg^{-1}, respectively). This is in accord with the main concept on ferralitic soils, that is, predominance of kaolinite, smaller presence of iron and aluminum oxides with minor proportions of other components in the clay fraction (IUSS Working Group WRB, 2014).

The mineralogical content of the studied soils was similar to those ferralitic soils (Latosols) of the central Brazilian Plateau that were studied by Vendrame et al. (2012). Those soils contained 243 ± 92 g kg^{-1} kaolinite, 71 ± 60 g kg^{-1} gibbsite, 60 ± 39 g kg^{-1} goethite and 40 ± 41 g kg^{-1} hematite. However, the iron contents in the Madagascar soils were lower than those observed in the central Brazilian Plateau but similar to other Brazilian tropical soils (Melfi et al., 1979), classified as hypo- to meso-ferric. In granite-derived soils of South Africa, Bühmann and Kirsten (1991) observed that kaolinite, halloysite, gibbsite and goethite were the most common secondary minerals. These authors emphasize the fact that kaolinite was the most common alteration product of granites and mafic rocks under most climatic conditions, from arid to humid. In West Africa, Dabin and Maignien (1979) found that kaolinite and illite were the main components of the ferralitic soils, however, the thickness of the oxic horizon and the losses of silicon and iron was less pronounced than for other tropical regions due to less current rainfall.

The R_{KGb} ratio of the studied soils (0.75 ± 0.25) was also very similar to the that of the Brazilian Latosols studied by Vendrame et al (2012) (R_{KGb} = 0.77 ± 0.3). Therefore, the variability of the kaolinite and gibbsite contents of the studied samples fairly well covered the variability of the mineralogical composition of highly weathered tropical soils. Therefore, the selected population of samples would be favorable to construct reliable calibrations with a limited number of samples.

4.2 Quantitative analysis of the mineralogy of ferralitic soils with chemometric methods

Infrared spectra of soils contain extensive information on soil minerals associated with vibrations of O-H, Al-O, Fe-O and Si-O groups. The main frequencies and wavelengths of spectral absorption in the MIR and Vis-NIR for major soil minerals, comprising quartz, clay minerals (kaolinite, smectite/illite), carbonates, aluminum (Al)/iron (Fe) oxyhydroxydes and Fe oxides, have been reviewed recently by Soriano-Disla et al. (2014). However, quantitative predictions of the mineralogical content (kaolinite, gibbsite, goethite, hematite) of soils using infrared spectroscopy are scarce.

Few studies have used infrared spectroscopic techniques as a tool for the quantifications of kaolinite in soils. A first attempt to determine the composition of mineral-organic mixes, made of pure minerals including kaolinite, illite and smectite, was carried out by Viscarra Rossel et al. (2006a). The prediction of the amount of kaolinite in the test mixtures were accurate (R^2 = 0.94; RPD = 4.1). Brown et al. (2006) were also able to predict kaolinite in a semi-quantitative manner (0-5 scale) using X-ray diffraction (XRD) as reference. The work

by Vendrame et al. (2012) is one of the first studies on tropical soils, where prediction of kaolinite content by NIRS was effective (R^2 = 0.82; RPD = 2.4). Our results (R^2 = 0.60; RPD = 1.6; Table 2), using a similar methodology, for the ferralitic soils of Madagascar are less promising than those of Vendrame et al. (2012) as they are slightly lower than what is considered acceptable according to Chang et al. (2001).

Results on the quantifications of gibbsite in soils are even scarcer than those for kaolinite. NIR-spectroscopy was used for quantitative analysis of the gibbsite of lateritic bauxite (Konrad et al., 2015), showing that it is an excellent method (R^2 = 0.99) and an efficient alternative to common X-ray methods at mining sites. However, except the work by Vendrame et al. (2012), we have not found other work using chemometric methods for quantifying soil gibbsite. For reference analyses, they used thermogravimetric analysis (TGA) and SA, and found better results for TGA (R^2 = 0.90; RPD = 3.2) than for SA (R^2 = 0.64; RPD = 1.7). Our results, using SA extraction for reference, are consistent with those of Vendrame et al. (2012), with R^2= 0.60 and RPD = 1.6 (Table 2).

The iron oxide content of soils has been predicted from different spectral regions of the Vis-NIR, based on characteristic absorption features at 550–650, 750–950, 1 406 and 2 449 nm (Summers et al., 2011). The reference analyses were carried out using total elemental analyses (Ben-Dor and Banin, 1994), SA extraction (Vendrame et al., 2012; this study) or CBD extraction method (Ben-Dor and Banin, 1994; Ben-Dor et al., 2008; Summers et al., 2011; this study) of which the CBD extraction method proved to be the most effective (Ben-Dor and Banin, 1994; this study, Table 2). Our prediction of the iron oxide content (R^2 = 0.80 and RPD = 2.2) of soils using CBD extraction was based solely on NIR (1100-2500 nm), while the other studies used Vis-NIR (350 or 400-2 500 nm). The resulting coefficient of determination was still comparable (R^2= 0.61-0.98) which is notable since the major absorption features of iron oxides appear generally in the Vis region (550–650 nm).

Quantitative analysis of the mineralogy of ferralitic soils with diagnostic absorption peaks has been of great concern for a long time. Except a few studies (Madeira et al., 1995), this methodology was rarely used due to the inhomogeneities of soil samples that preclude highly accurate quantitative analysis (White and Roth, 1986). In our study, this method, using the two diagnostic absorption peaks of kaolinite and gibbsite on the first derivative spectra, gave better results than those obtained previously with multivariate calibration on the whole spectra: the R^2_c between kaolinite or gibbsite contents and spectral data increased from 0.60 to 0.69 for kaolinite and from 0.60 to 0.71 for gibbsite; the R^2_v increased from 0.37 to 0.72 for kaolinite and from 0.51 to 0.72 for gibbsite.

The presence of interfering secondary peaks of other minerals in the diagnostic peak can also disrupt the quality of the results. The kaolinite spectrum is characterized by an absorption feature at approximately 2 200 nm, as well as illite or montmorillonite spectra (Dufréchou et al., 2015). The presence of significant levels of montmorillonite is unlikely in ferrallitic soils, but that of illite was observed (Dabin and Maignien, 1979). However, the peak of the kaolinite is generally located at around 2 205-2 208 nm, while the stronger peak of illite is located at smaller wavelength, i.e. 2 198-2 206 nm (Post and Noble, 1993). As in our study the peaks were always located at 2 206-2 208 nm, significant interference between kaolinite and illite was unlikely.

5 Final considerations and conclusions

Highly weathered ferralitic soils cover large areas in the tropics. The reactive mineral constituents of soils, i.e. clay minerals (kaolinite) and Al/Fe oxides (gibbsite, goethite, hematite), play a key role, with organic matter, in the physico-chemical functioning of soils.

Soil mineral composition (type, proportion, and concentration) determine soil properties, such as texture, structure, and CEC, and are responsible for P sorption (Soriano-Disla et al., 2014). The use of spectroscopy-based analysis to estimate this composition in weathered tropical soils can be useful to assist soil survey and group soils with similar characteristics. It is particularly relevant in poor countries, such as Madagascar, where soil surveys are incomplete and mostly developed for great scales and where rapid and more cost-effective methodologies are required for the assessment of soil quality indicators (Mairura et al., 2007).

While numerous studies have been conducted to quantify the soil organic matter with infrared spectral methods (see Soriano-Disla et al., 2014), research on soil mineralogy using this approach is still scarce. In our study, multivariate calibration on the whole spectra failed to give models of good quality to predict kaolinite and gibbsite: the iron oxide content using CBD extraction was the only one which could be predicted with this method. However, we showed that reliable spectroscopy-based analyses of soil mineralogy can be obtained with NIR-spectrometry using diagnostic absorption peaks of kaolinite and gibbsite. These results are encouraging for the development of similar studies on larger data sets.

Acknowledgements

This research was supported by Agropolis Fondation (France) under the reference ID 1001-009 through the « Investissements d'avenir » programme (Labex Agro: ANR-10-LABX-0001-01) and by Agropolis Fondation and CAPES (Brazil) under the reference ID

1002-006. We would like to thank Dr. B. Madari, from Embrapa, Brazil, for her useful comments and revision of the English.

References

Adamoli, J., Macedo, J., Azevedo, L.G., Madeira, J., 1985. Caracterização da região dos Cerrados, in, Goedert, W.J. (Ed.), Solos do Cerrado: tecnologias e estratégias de manejo, first ed. Nobel, São Paulo, pp. 33–74.

Ben-Dor, E., Banin, A., 1994. Visible and near-infrared (0.4-1.1 µm) analysis of arid and semiarid soils. Remote Sens. Environ. 48, 261-274.

Ben-Dor, E., Chabrillat, S., Demattê, J.A.M., Taylor, G.R., Hill, J., Whiting, M.L., Sommer, S., 2009. Using imaging spectroscopy to study soil properties. Remote Sens. Environ. 113, S38–S55.

Ben-Dor, E., Heller, D., Chudnovsky, A., 2008. A novel method of classifying soil profiles in the field using optical means. Soil Sci. Soc. Am. J. 72, 1113-1123.

Ben-Dor, E., Levin, N., Singer, A., Karnieli, A., Braun, O., Kidron, G.J., 2006. Quantitative mapping of the soil rubification process on sand dunes using an airborne hyperspectral sensor. Geoderma 131, 1–21.

Bond, W.J., Silander, J.A., Ranaivonasy, J., Ratsirarson, J., 2008. The antiquity of Madagascar's grasslands and the rise of C4 grassy biomes. J. Biogeogr. 35, 1743–1758.

Brown, D.J., Shepherd, K.D., Walsh, M.G., Mays, M.D., Reinsch, T.G., 2006. Global soil characterization with VNIR diffuse reflectance spectroscopy. Geoderma 132, 273–290.

Brunet, D., Barthès, B.G., Chotte, J.L., Feller, C., 2007. Determination of carbon and nitrogen contents in Alfisols, Oxisols and Ultisols from Africa and Brazil using NIRS analysis: Effects of sample grinding and set heterogeneity. Geoderma 139, 106–117.

Bühmann, C., Kirsten, W.F.A., 1991. The mineralogy of five weathering profiles developed from Archaean granite in the eastern Transvaal, Republic of South Africa. S. Afr. J. Plant Soil 8, 146–152.

Cécillon, L., Barthès, B.G., Gomez, C., Ertlen, D., Genot, V., Hedde, M., Stevens, A., Brun, J.J., 2009. Assessment and monitoring of soil quality using near-infrared reflectance spectroscopy (NIRS). Eur. J. Soil Sci. 60, 770–784.

Chang, C.W., Laird, D.A., Mausbach, M.J., Hurburgh, C.R., 2001. Near-infrared reflectance spectroscopy - principal components regression analyses of soil properties. Soil Sci. Soc. Am. J. 65, 480-490.

Collins, A.S., Windley, B.F., 2002. The tectonic evolution of central and northern Madagascar and its place in the final assembly of Gondwana. J. Geol. 110, 335-340.

Cornell, R.M., Schwertmann, U., 1996. The iron oxides: structure, properties, reactions, occurrence and uses. VCH Publishers, Weinheim.

CPCS, 1967. Classification des sols. Commission de Pédologie et de Cartographie des Sols, ENSA, Grignon.

Dabin, B., Maignien, R., 1979. Les principaux sols d'Afrique de l'Ouest et leurs potentialités agricoles. Cah. ORSTOM, série Pédol. 4, 235–257.

Demattê, J.A.M., da Silva Terra, F., 2014. Spectral pedology: a new perspective on evaluation of soils along pedogenetic alterations. Geoderma, 217, 190-200.

Dewitte, O., Jones, A., Spaargaren, O., Breuning-Madsen, H., Brossard, M., Dampha, A., Deckers, J., Gallali, T., Hallett, S., Jones, R., Kilasara, M., Le Roux, P., Michéli, E., Montanarella, L., Thiombiano, L., Van Ranst, E., Yemefack, M., Zougmore, R., 2013. Harmonisation of the soil map of Africa at the continental scale. Geoderma 211, 138–153.

Dufréchou, G., Grandjean, G., Bourguignon, A., 2015. Geometrical analysis of laboratory soil spectra in the short-wave infrared domain: Clay composition and estimation of the swelling potential. Geoderma 243–244, 92–107.

Eberhardt, D.N., Vendrame, P.R.S., Becquer, T., Guimarães, M.F., 2008. Influência da granulometria e da mineralogia sobre a retenção do fósforo em latossolos sob pastagens no cerrado. Rev. Bras. Cienc. Solo 32, 1009–1016.

Farmer, V.C., Russell, J.D., 1964. The infra-red spectra of layer silicates. Spectroc. Acta 20, 1149–1173.

IUSS Working Group WRB, 2014. World reference base for soil resources 2014 International soil classification system. World Soil Resources Reports 106, 1-203.

Janik, L.J., Merry, R.H., Skjemstad, J.O., 1998. Can mid infrared diffuse reflectance analysis replace soil extractions? Aust. J. Exp. Agric. 38, 681–696.

Jeanroy, E., Rajot, J.L., Pillon, P., Herbillon, A.J., 1991. Differential dissolution of hematite and goethite in dithionite and its implication on soil yellowing. Geoderma 50, 79–94.

Konrad, F., Stalder, R., Tessadri, R., 2015. Quantitative phase analysis of lateritic bauxite with NIR-spectroscopy. Miner. Eng. 77, 117–120.

Madari, B.E., Reeves III, J.B., Coelho, M.R., Machado, P.L.O.A., De-Polli, H., Coelho, R.M., Benites, V.M., Souza, L.F., McCarty, G.W., 2005. Mid- and near-infrared spectroscopic determination of carbon in a diverse set of soils from the Brazilian national soil collection. Spectrosc. Lett. 38, 721–740.

Madeira, J., Bédidi, A., Pouget, M., Cervelle, B., Flay, N., 1995. Spectral (MIR) determination of kaolinite and gibbsite contents in lateritic soils. Comptes Rendus Acad. Sci. Ser II-A 321, 119-128.

Mairura, F.S., Mugendi, D.N., Mwanje, J.I., Ramisch, J.J., Mbugua, P.K., Chianu, J.N. 2007. Integrating scientific and farmers' evaluation of soil quality indicators in Central Kenya. Geoderma 139, 134-143.

Malley, D.F., Martin, P.D., Ben-Dor, E., 2004. Application in analysis of soils. Near-infrared Spectrosc. Agric. 26, 729–784.

Mehra, O.P., Jackson, M., 1960. Iron oxide removal from soils and clays by a dithionite-citrate system buffered with sodium bicarbonate. Clays Clay Min. 7, 317–327.

Melfi, A.J., Pedro, G., Volkoff, B., 1979. Natureza e distribuição dos compostos ferríferos nos solos do Brasil. Rev. Bras. Cienc. Solo 3, 47–54.

Minasny, B., Hartemink, A.E., 2011. Predicting soil properties in the tropics. Earth-Sci. Rev. 106, 52-62.

Móron, A., Cozzolino, D., 2003. Exploring the use of near infrared reflectance spectroscopy to study physical properties and microelements in soils. J. Near Infrared Spectrosc. 11, 145–154.

Nocita, M., Stevens, A., Van Wesemael, B., Aitkenhead, M., Bachmann, M., Barthès, B., Ben Dor, E., Brown, D.J., Clairotte, M., Csorba, A., Dardenne, P., Demattê, J. A. M., Genot, V., Guerrero, C., Knadel, M., Montanarella, L., Noon, C., Ramirez-Lopez, L., Robertson, J., Sakai, H., Soriano-Disla, J.M., Shepherd, K.D., Stenberg, B., Towett, E.K., Vargas, R., Wetterlind, J., 2015. Soil spectroscopy: an alternative to wet chemistry for soil monitoring. Adv. Agron. 132, 139–159.

Nziguheba, G., Zingore, S., Kihara, J., Merckx, R., Njoroge, S., Otinga, A., Vandamme, E., Vanlauwe, B., 2015. Phosphorus in smallholder farming systems of sub-Saharan Africa : implications for agricultural intensification. Nutr. Cycl. Agroecosyst., 1-20. (On Line - DOI 10.1007/s10705-015-9729-y)

Post, J.L., Noble, P.N., 1993. The near-infrared combination band frequencies of dioctahedral smectites, micas, and illites. Clays Clay Min. 41, 639–644.

R Core Team, 2015. R: a language and environment for statistical computing. R Foundation for Statistical Computing, Vienna, Austria. https://www.R-project.org/.

Reatto, A., Bruand, A., Martins, E.S., Muller, F., Silva, E.M., Carvalho, O.A., Brossard, M., 2008. Variation of the kaolinite and gibbsite content at regional and local scale in Latosols of the Brazilian Central Plateau. C. R. Geosci. 340, 741–748.

Reatto, A., Bruand, A., Martins, E.S., Muller, F., Silva, E.M., Carvalho, O.A., Brossard, M., Richard, G., 2009. Development and origin of the microgranular structure in latosols of the Brazilian Central Plateau: significance of texture, mineralogy, and biological activity. Catena 76, 122–134.

Reeves III, J., McCarty, G., Mimmo, T., 2002. The potential of diffuse reflectance spectroscopy for the determination of carbon inventories in soils. Environ. Pollut. 116, 277–284.

Roederer, P., 1971. Les sols de Madagascar. Sciences de la Terre, Pédologie, 5. ORSTOM, Tananarive.

Santana, D.P., 1984. Soil formation in a toposequence of oxisols from Patos de Minas region, Minas Gerais, State, Brasil. Ph. D. Thesis. Purdue University, West Lafayette. 129 pp.

Schaefer, C.E.G.R., Fabris, J.D., Ker, J.C., 2008. Minerals in the clay fraction of Brazilian Latosols (Oxisols): a review. Clay Min. 43, 137–154.

Shepherd, K.D., Walsh, M.G., 2002. Development of reflectance spectral libraries for characterization of soil Properties. Soil Sci. Soc. Am. J. 66, 988.

Soriano-Disla, J.M., Janik, L.J., Viscarra Rossel, R.A., MacDonald, L.M., McLaughlin, M.J., 2014. The performance of visible, near-, and mid-infrared reflectance spectroscopy for prediction of soil physical, chemical, and biological properties. Appl. Spectrosc. Rev. 49, 139–186.

Stenberg, B., Viscarra Rossel, R.A., Mouazen, A.M., Wetterlind, J., 2010. Chapter five - visible and near infrared spectroscopy in soil science. Adv. Agron. 107, 163-215.

Summers, D., Lewis, M., Ostendorf, B., Chittleborough, D., 2011. Visible near-infrared reflectance spectroscopy as a predictive indicator of soil properties. Ecol. Indic. 11, 123–131.

Vendrame, P.R.S., Brito, O.R., Martins, E.S., Quantin, C., Guimarães, M.F., Becquer, T., 2013. Acidity control in Latosols under long-term pastures in the Cerrado region, Brazil. Soil Res. 51, 253–261.

Vendrame, P.R.S., Marchão, R.L., Brunet, D., Becquer, T., 2012. The potential of NIR spectroscopy to predict soil texture and mineralogy in Cerrado Latosols. Eur. J. Soil Sci. 63, 743–753.

Viscarra Rossel, R.A., 2011. Fine-resolution multiscale mapping of clay minerals in Australian soils measured with near infrared spectra. J. Geophys. Res. 116, 1–15.

Viscarra Rossel, R.A., Cattle, S.R., Ortega, A., Fouad, Y., 2009. In situ measurements of soil colour, mineral composition and clay content by vis-NIR spectroscopy. Geoderma 150, 253–266.

Viscarra Rossel, R.A., McGlynn, R.N., McBratney, A.B., 2006a. Determining the composition of mineral-organic mixes using UV-vis-NIR diffuse reflectance spectroscopy. Geoderma 137, 70–82.

Viscarra Rossel, R.A., Walvoort, D.J.J., McBratney, A.B., Janik, L.J., Skjemstad, J.O., 2006b. Visible, near infrared, mid infrared or combined diffuse reflectance spectroscopy for simultaneous assessment of various soil properties. Geoderma 131, 59–75.

White, J.L., Roth, C.B., 1986. Infrared spectrometry, in: Klute, A. (Ed.), Methods of Soil Analysis: Part 1. Physical and Mineralogical Methods, 2nd edition. ASA and SSSA, Madison, pp. 291-330.